

Geophysical Research Letters

RESEARCH LETTER

10.1029/2020GL090559

Key Points:

- We matched profiling float trajectories with ocean-color satellite observations of coccolithophore blooms
- Two simple bio-optical indices permitted successful identification of coccolithophore blooms from floats in the Southern Ocean
- A method for identifying coccolithophore blooms at the global scale is proposed using regional thresholds of bio-optical float measurements

Supporting Information:

- Supporting Information S1

Correspondence to:

L. Terrats,
louis.terrats@gmail.com

Citation:

Terrats, L., Claustre, H., Cornec, M., Mangin, A., & Neukermans, G. (2020). Detection of coccolithophore blooms with BioGeoChemical-Argo floats. *Geophysical Research Letters*, 47, e2020GL090559. <https://doi.org/10.1029/2020GL090559>

Received 27 AUG 2020

Accepted 2 NOV 2020

Accepted article online 9 NOV 2020

©2020. The Authors.

This is an open access article under the terms of the Creative Commons Attribution License, which permits use, distribution and reproduction in any medium, provided the original work is properly cited.

Detection of Coccolithophore Blooms With BioGeoChemical-Argo Floats

L. Terrats^{1,2} , H. Claustre¹ , M. Cornec¹ , A. Mangin², and G. Neukermans^{3,4} 

¹Sorbonne Université, CNRS, Laboratoire d'Océanographie de Villefranche, LOV, Villefranche-sur-Mer, France,

²ACRI-ST, Sophia Antipolis, France, ³Biology Department, MarSens Research Group, Ghent University, Ghent, Belgium,

⁴Flanders Marine Institute (VLIZ), InnovOcean site, Ostend, Belgium

Abstract Coccolithophores (calcifying phytoplankton) form extensive blooms in temperate and subpolar oceans as evidenced from ocean-color satellites. This study examines the potential to detect coccolithophore blooms with BioGeoChemical-Argo (BGC-Argo) floats, autonomous ocean profilers equipped with bio-optical and physicochemical sensors. We first matched float data to ocean-color satellite data of calcite concentration to select floats that sampled coccolithophore blooms. We identified two floats in the Southern Ocean, which measured the particulate beam attenuation coefficient (c_p) in addition to two core BGC-Argo variables, Chlorophyll-*a* concentration ([Chl-*a*]) and the particle backscattering coefficient (b_{bp}). We show that coccolithophore blooms can be identified from floats by distinctively high values of (1) the b_{bp}/c_p ratio, a proxy for the refractive index of suspended particles, and (2) the $b_{bp}/[\text{Chl-}a]$ ratio, measurable by any BGC-Argo float. The latter thus paves the way to global investigations of environmental control of coccolithophore blooms and their role in carbon export.

Plain Language Summary Coccolithophores are a group of phytoplankton that form an armor of calcite plates. Coccolithophores may form intense blooms which can be identified from space by so-called ocean-color satellites, providing global images of the color of the surface ocean. BioGeoChemical-Argo (BGC-Argo) floats, robots profiling down to 2,000 m with a variety of physicochemical and bio-optical sensors, present an increasingly attractive and cost-effective platform to study phytoplankton blooms and their impact on oceanic biogeochemical cycles. We show that coccolithophore blooms can be detected by BGC-Argo floats with high confidence, hence providing a new way to study them at the global scale as well as their role in sinking carbon.

1. Introduction

Detecting major phytoplankton groups is essential to improve our understanding of the global biogeochemical cycles. One such group is the coccolithophores, calcifying phytoplankton which form calcite platelets called coccoliths. The coccolithophore species *Emiliania huxleyi* forms extensive blooms in the temperate and subpolar surface ocean, characterized by detachment and overproduction of coccoliths in the bloom decline phase (Balch et al., 1991, 1996). The accumulation of these high-refractive-index calcite particles increases the light backscattered from the ocean surface and colors the water milky-turquoise (Holligan et al., 1983).

Ocean-color satellites can detect these milky-turquoise coccolithophore bloom waters, and remote sensing algorithms have been set up to quantify the associated concentration of particulate inorganic carbon ([PIC] in mmol m^{-3}) (Balch et al., 2005; Gordon et al., 2001). Remotely sensed [PIC] has been used to investigate regional, seasonal, and interannual variabilities of coccolithophore blooms at global scale (Hopkins et al., 2015, 2019) and to locate coccolithophore blooms to guide ship-based sampling (Garcia et al., 2011). Ship-based measurements of coccolithophore blooms are valuable to calibrate satellite algorithms and investigate the influence of coccolithophore blooms on ocean biogeochemistry (Balch et al., 2005, 2016; Garcia et al., 2011). However, ship missions cover limited spatiotemporal scales and satellites are limited to surface waters and clear-sky conditions, creating observational gaps, particularly in high-latitude regions.

BioGeoChemical-Argo (BGC-Argo) floats, free-drifting autonomous ocean profilers equipped with bio-optical and physicochemical sensors, present an increasingly attractive platform to study environmental control and biogeochemical processes related to phytoplankton blooms (Briggs et al., 2020;

Lacour et al., 2015; Mignot et al., 2018). They provide observations at unparalleled temporal and vertical scales and fill observational gaps in undersampled regions, such as high-latitude waters (Claustre et al., 2020). Among the core variables measured by BGC-Argo floats are the particulate backscattering coefficient (b_{bp} , in m^{-1}), a proxy for suspended particle concentration, and Chlorophyll-*a* fluorescence (FChl-*a*) from which one can derive the concentration of Chlorophyll-*a* ([Chl-*a*] in $mg\ m^{-3}$), the primary photosynthetic pigment in phytoplankton cells. Additionally, few floats are equipped with a beam transmissometer, which measures the particulate beam attenuation coefficient (c_p , in m^{-1}), another proxy for suspended particle concentration.

The objective of this study is to examine if bio-optical measurements from BGC-Argo floats can be used to detect coccolithophore blooms. A first candidate optical property is the b_{bp}/c_p ratio, a proxy for the bulk refractive index of suspended particles (Twardowski et al., 2001). Indeed, ship-based studies have shown that the decline phase of *E. huxleyi* blooms is characterized by large concentrations of shed coccoliths (Balch et al., 1991), non-chlorophyllous, high-refractive-index particles, resulting in increased b_{bp}/c_p (Garcia et al., 2011). However, only a limited number of floats measure c_p . Therefore, we also examine the potential to identify blooms from a second candidate property, the $b_{bp}/[Chl-a]$ ratio, which can be measured by any BGC-Argo float.

2. Materials and Methods

We focused on BGC-Argo float trajectories in temperate and subpolar open-ocean waters (i.e., $>35^\circ N$ and $>35^\circ S$) during the coccolithophore growing seasons (i.e., spring and summer). We matched each profile of the floats with concurrent ocean-color satellite data. Using the satellite [PIC] time series at each profile location, we set up a technique to decide if the profile was located in a coccolithophore bloom or not and then tested for significant differences in the b_{bp}/c_p ratio and the $b_{bp}/[Chl-a]$ ratio between profiles in coccolithophore bloom and non-bloom conditions.

2.1. Float Measurements and Derived Variables

We first searched the BGC-Argo float database for floats equipped with a backscattering and chlorophyll-*a* fluorescence sensor, as well as a beam transmissometer. We identified two floats drifting in the subpolar Southern Ocean. They operated at a daily frequency and were identified by their World Meteorological Organization numbers (WMO) as 6901583 and 6902738. Afterward, we expanded our analyses to every float equipped with backscattering and chlorophyll-*a* fluorescence sensors.

The ECO Triplet (Three Channel Sensor; WET Labs, Inc., USA) measures FChl-*a* and the fluorescence of Colored Dissolved Organic Matter (CDOM) at excitation/emission wavelengths of 470/695 and 370/460 nm, respectively, and the angular scattering coefficient of particles at 700 nm and an angle of 124° , from which we derived b_{bp} at 700 nm (Boss & Pegau, 2001; Schmechtig et al., 2018). We corrected b_{bp} and FChl-*a* profiles for out-of-range values and the sensor drift over time following quality control procedures (Bellacicco et al., 2019). The C-Rover beam transmissometer (WET Labs, Inc., USA) measures the attenuation of light by particles at 660 nm (c_p in m^{-1}), which is almost entirely attributable to light scattering by particles at that wavelength (Loisel & Morel, 1998). The vertical position of the transmissometer causes sinking material to accumulate progressively on the detection window over time, resulting in a drift of c_p values (Bishop & Wood, 2009). The drift was corrected by aligning c_p vertical profiles such that b_{bp}/c_p equalled 0.02 at 1000 m. Our sensitivity analysis showed that c_p values at the surface did not vary significantly when the ratio b_{bp}/c_p ranged from 0.01 to 0.03 at 1,000 m (see Table S1 and Text S1 in the supporting information).

The bio-optical values transiently increase when particle aggregations or mesopelagic organisms pass in front of the detector, which creates spikes in bio-optical profiles (Briggs et al., 2011; Haëntjens et al., 2020). We removed these spikes by smoothing the bio-optical profiles using a 5-point moving median filter followed by a 7-point moving average filter (Briggs et al., 2011). Finally, we visually inspected the profiles on a case-by-case basis.

We converted FChl-*a* to [Chl-*a*] as follows: (i) FChl-*a* was corrected for the Non-Photochemical Quenching (NPQ), a photo-protection mechanism that depresses the FChl-*a* per unit of [Chl-*a*] (or b_{bp}) with diurnal increases in irradiance, through a modification of the method of Xing et al. (2018) (see Text S2 and

Figures S1 and S2 in the supporting information for further details on this method), (ii) then converted to [Chl-*a*] with the factory calibration coefficient, (iii) and finally adjusted with satellite [Chl-*a*] to compensate for spatial variations in the calibration coefficient revealed by Roesler et al. (2017) (see Text S2 in the supporting information).

We estimated the mixed layer depth (MLD) with the algorithm of Holte and Talley (2009) that relies on temperature, salinity, and density profiles. This method considers physical features, such as the vertical density-compensation, and provides a more accurate estimate of the MLD in high-latitude waters compared to threshold and gradient approaches (Holte et al., 2017; Holte & Talley, 2009).

2.2. Satellite Data

Daily-merged ocean-color satellite data were downloaded from the GlobColour project (<ftp://ftp.hermes.acri.fr>) with a spatial resolution of 4 km. We described the dynamic of coccolithophore blooms with the [PIC] satellite product using the state-of-the-art retrieval algorithm of Mitchell et al. (2017) (see Figure 8c in Mitchell et al., 2017). We further use %PIC defined as follows:

$$\%PIC = \frac{[PIC]}{[PIC] + [POC]} \times 100, \quad (1)$$

where [POC] is the concentration of particulate organic carbon using the retrieval algorithm of Stramski et al. (2008). In coccolithophore blooms, we appraised the reliability of the band-difference algorithm of Mitchell et al. (2017) to perceive changes in b_{bp} by comparing [PIC] to the satellite b_{bp} values from the inverse model of Maritorena and Siegel (2005). Finally, we reported the GlobColour [Chl-*a*] product which is derived from various algorithms optimized for different water types (i.e., Antoine & Morel, 1996; Gohin et al., 2002; Hu et al., 2012; O'Reilly et al., 1998, 2000), and we removed the estimates in coccolithophore blooms where ocean-color satellite retrievals of [Chl-*a*] are biased (Balch et al., 1989).

2.3. Matchups Between Satellite and Float Data

The thickness of the surface ocean layer detected by satellites can be derived from vertical profiles of downward irradiance acquired by BGC-Argo floats. Unfortunately, 67% of irradiance profiles of floats 6901583 and 6902738 were categorized as “probably bad” quality records following the criteria of Organelli et al. (2016) and failed to meet the quality standards for radiometric applications. Therefore, we defined the surface layer sensed by ocean-color satellites as the first 15 m.

Bailey and Werdell (2006) defined matchup criteria between satellite and in situ data for the sake of validating ocean-color satellite radiometric products, which requires that the spatial and temporal difference in acquisition be as small as possible (5×5 pixel box at native resolution, narrow time window of <3 h). Here, the purpose of matching satellite and in situ data was to obtain a continuous gap-free time series of satellite data corresponding to the float trajectory. In persistently cloudy areas such as the Southern Ocean, this implies data averaging over larger spatial and temporal scales until a gap-free time series is achieved (e.g., Haëntjens et al., 2017). Our analyses showed that the optimal configuration to achieve a continuous time series of ocean-color satellite data matched to float data was a 9-day average of a 5×5 pixel box of 4 km resolution GlobColour satellite products (Figure S4 and Text S4 in the supporting information). In this configuration, the spatiotemporal variability of satellite-derived [PIC] was within $10 \pm 12\%$, indicating acceptable heterogeneity.

2.4. Detection of Coccolithophore Blooms With Satellite Data

To determine if a profile was located in a coccolithophore bloom, we extracted the time series of satellite [PIC] at each profile location. The bloom period was then defined using the algorithm of Hopkins et al. (2015) that estimates bloom start and end dates from [PIC] time series. To further improve the detection of coccolithophore blooms, we added the constraints that [PIC] exceeded 0.7 mmol m^{-3} and that %PIC exceeded 10%. This modified method compared favorably to occurrences of coccolithophore blooms reported in situ by Read et al. (2007) (see Figure S6 in the supporting information).

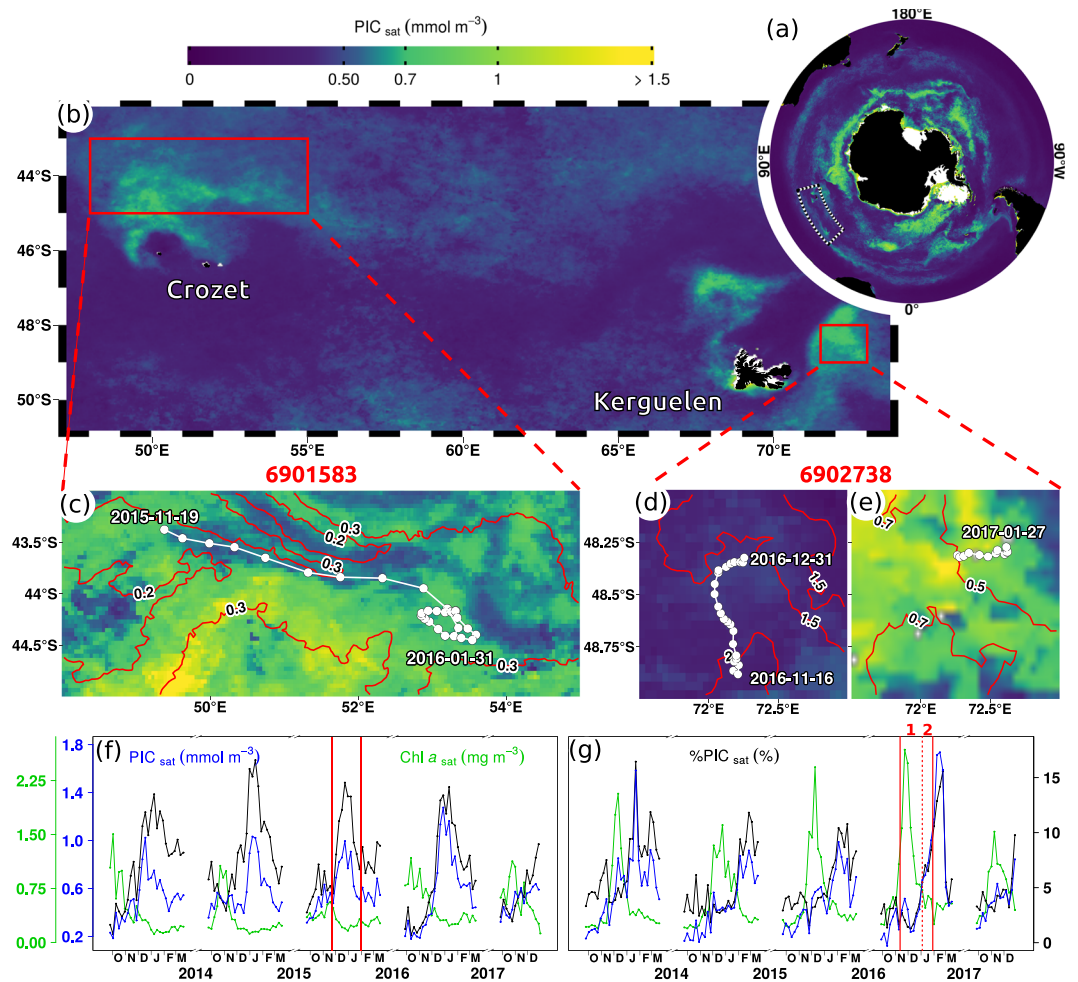


Figure 1. Float trajectories and coccolithophore bloom occurrences. (a) Summer climatology of satellite [PIC] (2012–2018) showing the Great Calcite Belt and (b) high-[PIC] patches in the study area. Red rectangles outline float sampling zones. Trajectories of floats 6901583 (c) and 6902738 during (d) the Period 1 of high [Chl-*a*] and (e) the Period 2 of increasing [PIC]. Background maps are satellite [PIC] averaged over the duration of float operations. Red lines correspond to isolines of satellite [Chl-*a*], and concurrent [Chl-*a*] maps are displayed on Figure S8 in the supporting information. (f, g) Area-averaged time series of [PIC], [Chl-*a*] and %PIC for both sampling zones, i.e., (f) is the time series for the area shown in (c) and (g) for (d)/(e). Vertical red lines indicate periods sampled by floats, and the dashed line separates Periods 1 and 2.

2.5. Statistical Analysis

Differences in b_{bp}/c_p and $b_{bp}/[Chl-a]$ between coccolithophore bloom and non-bloom conditions were evaluated with the Kruskal-Wallis test (i.e., one-way ANOVA on ranks).

To detect coccolithophore blooms with BGC-Argo floats, we set up a method based on b_{bp}/c_p and $b_{bp}/[Chl-a]$ thresholds derived from a Receiver Operating Characteristic (ROC) analysis (Woodward, 1953). The ROC analysis estimates the threshold value that optimally discriminates between coccolithophore bloom and non-bloom condition by maximizing the sensitivity (i.e., the proportion of coccolithophore bloom cases correctly identified) and the specificity (i.e., the proportion of non-bloom cases correctly identified).

3. Results and Discussion

3.1. BGC-Argo Float Trajectories in Zones of Coccolithophore Blooms

Both floats operated in the Great Calcite Belt, a large band of elevated [PIC] in the Southern Ocean in Austral summer (Figure 1a) resulting from coccolithophore blooms (Balch et al., 2011, 2016; Garcia et al., 2011;

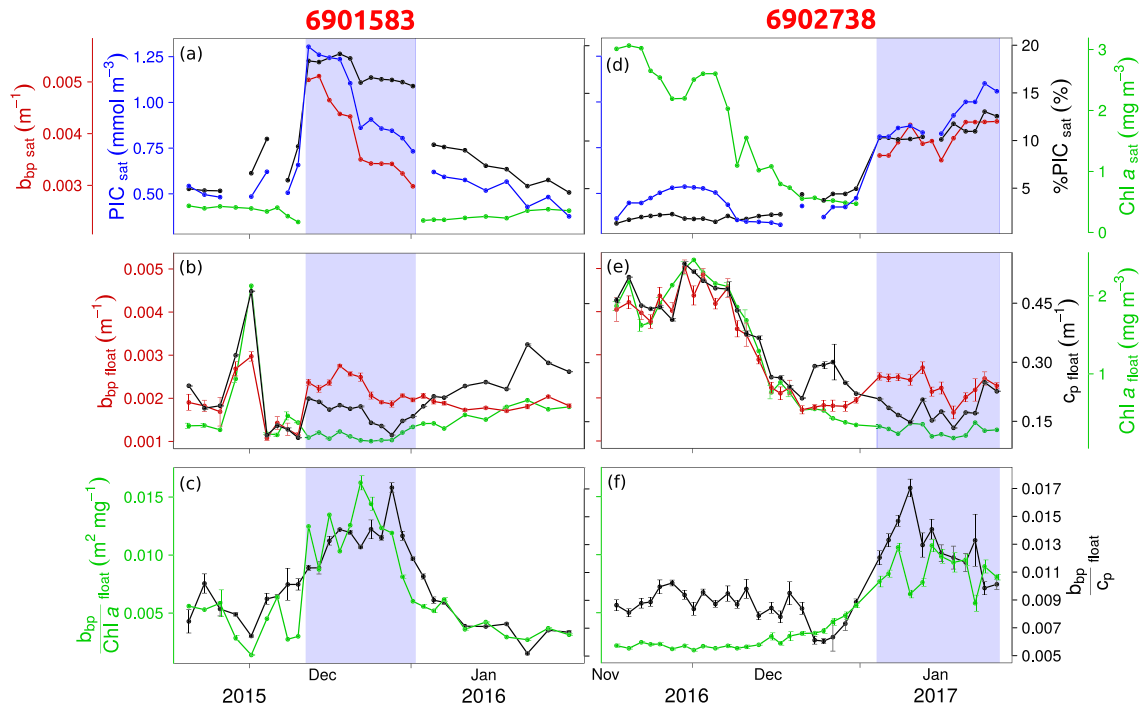


Figure 2. Optical measurements and satellite products during the operation of float 6901583 (a–c) and 6902738 (d–f). Time series of (a,d) [PIC], %PIC, [Chl-*a*], and b_{bp} measured by satellites; (b,e) b_{bp} , c_p , and [Chl-*a*] measured by floats; (c,f) $b_{bp}/[Chl-a]$ and b_{bp}/c_p measured by floats. Blue bands delineate the coccolithophore bloom period identified by the satellite detection method. Error bars indicate the standard deviation from the surface average.

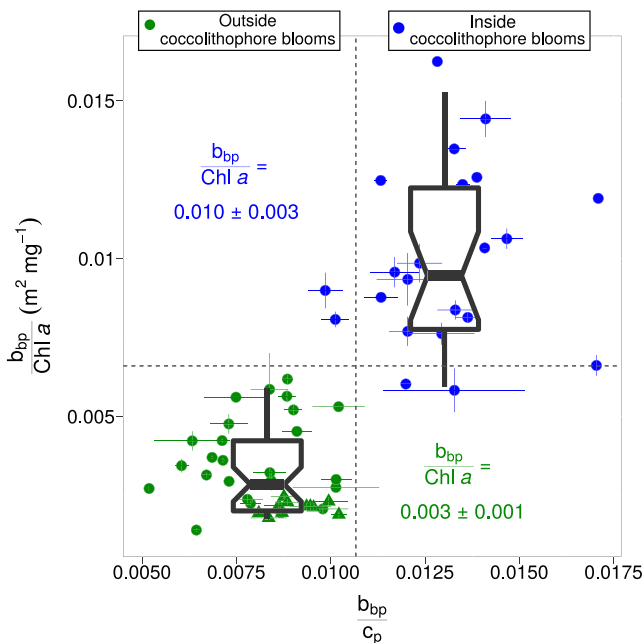


Figure 3. Optical ratios inside (blue dots) and outside (green dots) coccolithophore blooms sampled by floats 6901583 and 6902738. The dashed lines are the b_{bp}/c_p and $b_{bp}/[Chl-a]$ thresholds 0.011 and $0.007 \text{ m}^2 \text{ mg}^{-1}$, respectively, that best discriminate coccolithophore blooms from non-bloom cases.

Holligan et al., 2010). Float 6901583 drifted north of Crozet Islands and float 6902738 drifted east of Kerguelen Islands. Both zones have high summer [PIC] (Figures 1b, 1f, and 1g) caused by coccolithophore blooms dominated by *E. huxleyi* (Mohan et al., 2008; Patil et al., 2017; Read et al., 2007; Rembauville et al., 2016), giving the milky-turquoise ocean-color characteristic during float sampling (Figure S7 in the supporting information). Float 6901583 drifted on the northern edge of a coccolithophore bloom (Figure 1c), and float 6902738 near the core of a coccolithophore bloom (Figure 1e). The coccolithophore bloom detection method proposed in this study from time series analyses of satellite [PIC] showed that both floats operated throughout a coccolithophore bloom (Figures 2a and 2d).

Float 6902738 also sampled a bloom of non-calcifying phytoplankton, as evidenced from the high [Chl-*a*] values observed from space (Figures 1d and 2d) and by the float (Figure 2e). This pattern, of successive blooms of non-calcifying and calcifying phytoplankton throughout Austral spring and summer, appears to repeat itself on an annual basis as observed from ocean-color satellites time series from recent years (Figure 1g). Ship-based work in this area also confirmed a successional pattern, with a diatom bloom preceding an *E. huxleyi* bloom (Rembauville et al., 2016).

3.2. BGC-Argo Float Data in Coccolithophore Blooms

Both floats captured the evolution of a summer coccolithophore bloom, evidenced by satellite [PIC] that perceive changes in coccolith concentrations in accordance with satellite b_{bp} ($r^2 = 0.82$ between [PIC] and b_{bp} inside coccolithophore blooms on Figures 2a and 2d). Compared to

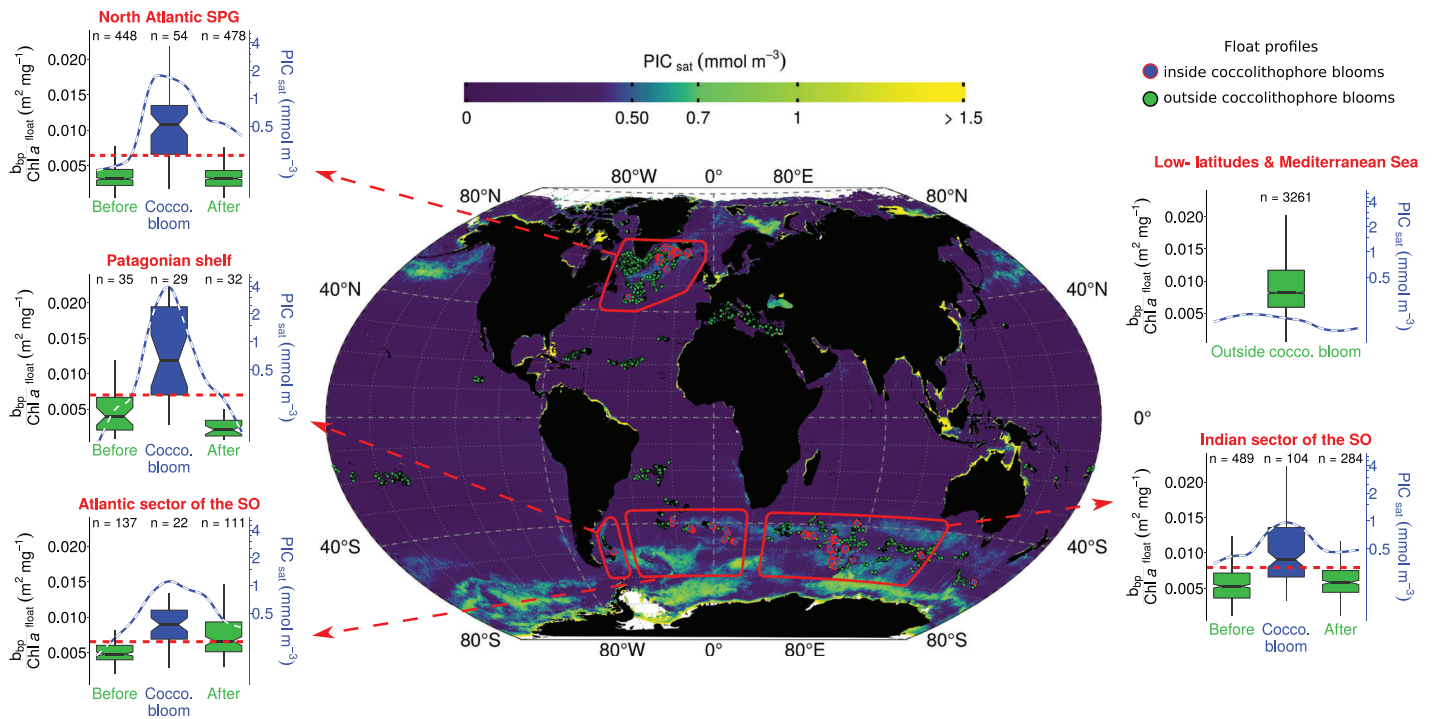


Figure 4. Detection of coccolithophore blooms with $b_{bp}/[Chl-a]$ thresholds. The map reveals locations of profiles inside coccolithophore blooms detected by satellites. The background map is the summer climatology (2012–2018) of satellite [PIC] for each hemisphere. Boxplots show distributions of $b_{bp}/[Chl-a]$ before, during, and after coccolithophore blooms in four temperate and subpolar regions identified with red polygons on the map, and in low-latitudes (i.e., $<35^\circ$) and Mediterranean Sea where no coccolithophore bloom was detected. Horizontal red dashed lines are the $b_{bp}/[Chl-a]$ thresholds reported in Table 1. Blue lines are [PIC].

coccolithophore blooms along the Patagonian Shelf (Garcia et al., 2011) or in the Subpolar Atlantic (Balch et al., 1996) where [PIC] can reach over 10 mmol m^{-3} , the coccolithophore blooms sampled in this study are of moderate intensity, as revealed by average [PIC] of $0.97 \pm 0.17 \text{ mmol m}^{-3}$ (Figures 2a and 2d).

The coccolithophore bloom period coincides with elevated values of $b_{bp}/[Chl-a]$ and b_{bp}/c_p measured by floats (Figures 2c and 2f), compared to values outside the bloom period. The mean value of the b_{bp}/c_p ratio in coccolithophore blooms equalled 0.013 ± 0.002 , which is close to the value of 0.01 reported by Balch et al. (1996), and significantly higher than the value of 0.008 ± 0.001 outside coccolithophore blooms ($p < 10^{-2}$). The bulk refractive index retrieved from the mean b_{bp}/c_p (ratio as a proxy for the backscattering ratio) in coccolithophore blooms equalled 1.13 (Twardowski et al., 2001), which is intermediate between a pure population of phytoplankton cells (1.05: Bricaud et al., 1988) and calcite particles (1.2: Lide, 1997). Furthermore, the mean $b_{bp}/[Chl-a]$ ratio in coccolithophore blooms sampled by floats 6901583 and 6902738 was 0.012 ± 0.003 and $0.009 \pm 0.002 \text{ m}^2 \text{ mg}^{-1}$, respectively. These values in coccolithophore blooms are roughly three times higher than the corresponding mean values outside coccolithophore blooms, respectively, 0.004 ± 0.001 and $0.003 \pm 0.001 \text{ m}^2 \text{ mg}^{-1}$ ($p < 10^{-2}$). These observations are consistent with increased backscattering owing to non-chlorophyllous, high-refractive-index particles, such as coccoliths. Both optical ratios, b_{bp}/c_p and $b_{bp}/[Chl-a]$, thus allowed successful discrimination of coccolithophore blooms (Figures 2c and 2f), even in these blooms of moderate intensity.

ROC analyses revealed threshold values for the b_{bp}/c_p and $b_{bp}/[Chl-a]$ ratios of 0.011 and $0.007 \text{ m}^2 \text{ mg}^{-1}$, respectively, that allowed optimal discrimination between coccolithophore bloom and non-bloom conditions (Figure 3). Each threshold correctly identified 91% of coccolithophore bloom and 100% of non-bloom cases. Discrimination between bloom and non-bloom conditions using either the b_{bp}/c_p or the $b_{bp}/[Chl-a]$ ratio thus rendered similar statistics for sensitivity and specificity. This offers the possibility to extend our analysis to the global scale, as all BGC-Argo floats are capable of measuring the $b_{bp}/[Chl-a]$ ratio while only few floats measure c_p .

Table 1
List of $b_{bp}/[Chl-a]$ and b_{bp} Thresholds for Temperate and Subpolar Regions and Their Performances to Detect Coccolithophore Blooms (i.e., Sensitivity and Specificity)

| Regions | Thresholds | | Performances (%) | |
|---------------------------------------|------------------------------------|-----------------------|------------------|-------------|
| | $b_{bp}/[Chl-a]$ ($m^2 mg^{-1}$) | b_{bp} (m^{-1}) | Sensitivity | Specificity |
| North Atlantic subpolar gyre | 0.0063 | 0.0033 | 74 | 99 |
| Patagonian shelf | 0.0069 | 0.0035 | 72 | 100 |
| Indian sector of the Southern Ocean | 0.0078 | 0.0019 | 60 | 98 |
| Atlantic sector of the Southern Ocean | 0.0064 | 0.0021 | 73 | 94 |
| Total | | | 67 | 98 |

3.3. Toward a Global Detection of Coccolithophore Blooms With BGC-Argo Floats

Using global observations of satellite [PIC], we identified 209 float profiles inside coccolithophore blooms and 5,330 outside blooms (Figure 4). Profiles associated with coccolithophore blooms were systematically recorded in temperate and subpolar waters (i.e., Southern Ocean and North Atlantic subpolar gyre), where *E. huxleyi* generally dominates coccolithophore populations (Balch et al., 1996, 2019; Patil et al., 2017; Poulton et al., 2011). In those waters, a regional analysis of the $b_{bp}/[Chl-a]$ ratio revealed significantly higher values inside coccolithophore blooms ($p < 10^{-5}$), consistent with observations from the two floats in the Southern Ocean (section 3.2). Thresholds for $b_{bp}/[Chl-a]$ ranged from $0.0063 m^2 mg^{-1}$ in the North Atlantic subpolar gyre to $0.0078 m^2 mg^{-1}$ in the Indian sector of the Southern Ocean (Table 1). Regional differences in $b_{bp}/[Chl-a]$ thresholds can be expected owing to differences in backscattering properties of coccolithophore blooms (e.g., the ratio of free to attached coccoliths, Balch et al., 1999, or the morphotype of coccoliths, Neukermans & Fournier, 2018), in regional variability in background b_{bp} associated with non-algal material (Bellacicco et al., 2019; Zhang et al., 2020), or in phytoplankton community composition and physiology (Barbieux et al., 2018; Cetinić et al., 2015).

Occasionally, high values of $b_{bp}/[Chl-a]$ are found in waters where no coccolithophore blooms were detected, such as the Mediterranean Sea and low-latitude waters (latitudes $<35^\circ$). In these waters, elevated values of $b_{bp}/[Chl-a]$ were generally associated with low values of $[Chl-a]$, rather than high values of b_{bp} , typical for coccolithophore blooms (Figure S9). We therefore improved the accuracy of the bloom detection method based on $b_{bp}/[Chl-a]$ by adding thresholds on b_{bp} , derived from ROC analysis on the profiles with elevated $b_{bp}/[Chl-a]$ (i.e., $b_{bp}/[Chl-a]$ above thresholds).

Combining $b_{bp}/[Chl-a]$ and b_{bp} thresholds allows the method to detect the predominance of non-chlorophyllous high-refractive-index particles that are abundant enough to intensely backscatter the light, which are conditions reported in coccolithophore blooms of *E. huxleyi* identified here by satellite [PIC]. With the $b_{bp}/[Chl-a]$ and b_{bp} thresholds listed on Table 1, the method successfully identified nearly three-quarter of coccolithophore bloom cases in all temperate and subpolar regions except in the Indian sector of the Southern Ocean, and greatly differentiated bloom from non-bloom cases as illustrated by high values of specificity (Table 1). The combination of $b_{bp}/[Chl-a]$ and b_{bp} , acquired by all BGC-Argo floats, thus allows the effective detection of coccolithophore blooms in situ at the global scale.

4. Conclusions

In this study, ocean-color satellite observations of coccolithophore blooms were matched with bio-optical measurements from BGC-Argo floats to test the feasibility of developing a float-based detection method for coccolithophore blooms. A spatiotemporal analysis of bio-optical observations from two floats in the Southern Ocean reveal significant increases in both b_{bp}/c_p and $b_{bp}/[Chl-a]$ in coccolithophore blooms. These increases are consistent with accumulations of coccoliths; non-chlorophyllous, high-refractive-index particles, typically associated with coccolithophore blooms of *E. huxleyi*. Since only a limited number of BGC-Argo floats measure c_p , we developed a detection method based on measurements of b_{bp} and $[Chl-a]$ alone, which are measured by all BGC-Argo floats with global distribution. We conclude that coccolithophore blooms can be successfully identified from floats using regional thresholds on $b_{bp}/[Chl-a]$ and b_{bp} .

This opens perspectives for global-scale studies of coccolithophore blooms with the global array of BGC-Argo floats, expected to expand to thousand floats in the near future (Claustre et al., 2020). Whereas ocean-color satellites offer global-scale observations of coccolithophore blooms in the surface ocean in cloud-free conditions, floats extend our view of carbon particles down to 1,000 m deep, complementing the observational dimensions covered by satellites. Future work will include observations from the subsurface ocean accessible by these floats, which offer the potential to investigate the global impact of coccolithophore blooms on ocean biogeochemistry as their role in sinking carbon to the deep ocean.

Conflict of Interest

The authors declare no conflict of interest.

Data Availability Statement

The data supporting the conclusions of this study are freely available at <https://doi.org/10.17882/76521>, and all BGC-Argo data are available at <ftp://ftp.ifremer.fr/ifremer/argo/dac/>. These data were collected and made freely available by the International Argo Program and the national programs that contribute to it (<http://www.argo.ucsd.edu>, <http://argo.jcommops.org>).

Acknowledgments

This study is a contribution to the following projects: remOcean (European Research Council, Grant agreement 246777); REFINE (European Research Council, Grant agreement 834177); SOCLIM (BNP Foundation); BGC-Argo-France (CNES-TOSCA); and NAOS (French Equipement d'avenir programme, Grant ANR J11R107-F). The Argo Program is part of the Global Ocean Observing System. Griet Neukermans was supported by a European Union Horizon 2020 Marie Skłodowska-Curie grant (no. 749949). Louis Terrats was supported by a CIFRE fellowship funded by ACRI-st (no. 2018/1815). The authors received several helpful suggestions for improving this manuscript from Catherine Mitchell and one anonymous reviewer, and their help is gratefully acknowledged. We thank A. Poteau, R. Sauzède, and C. Schmechtig for BGC-Argo data management and L. Beaufort, N. Briggs, and H. Loisel for fruitful discussions.

References

- Antoine, D., & Morel, A. (1996). Oceanic primary production: 1. Adaptation of a spectral light-photosynthesis model in view of application to satellite chlorophyll observations. *Global Biogeochemical Cycles*, *10*(1), 43–55. <https://doi.org/10.1029/95GB02831>
- Bailey, S. W., & Werdell, P. J. (2006). A multi-sensor approach for the on-orbit validation of ocean color satellite data products. *Remote Sensing of Environment*, *102*(1–2), 12–23. <https://doi.org/10.1016/j.rse.2006.01.015>
- Balch, W. M., Drapeau, D. T., Bowler, B. C., Lyczkowski, E., Booth, E. S., & Alley, D. (2011). The contribution of coccolithophores to the optical and inorganic carbon budgets during the Southern Ocean gas exchange experiment: New evidence in support of the “Great Calcite Belt” hypothesis. *Journal of Geophysical Research*, *116*, C00F06. <https://doi.org/10.1029/2011JC006941>
- Balch, W. M., Gordon, H. R., Bowler, B. C., Drapeau, D. T., & Booth, E. S. (2005). Calcium carbonate measurements in the surface global ocean based on moderate-resolution imaging spectroradiometer data. *Journal of Geophysical Research*, *110*, C07001. <https://doi.org/10.1029/2004JC002560>
- Balch, W. M., Bates, N. R., Lam, P. J., Twining, B. S., Rosengard, S. Z., Bowler, B. C., et al. (2016). Factors regulating the Great Calcite Belt in the Southern Ocean and its biogeochemical significance. *Global Biogeochemical Cycles*, *30*, 1124–1144. <https://doi.org/10.1002/2016GB005414>
- Balch, W. M., Bowler, B. C., Drapeau, D. T., Lubelczyk, L. C., Lyczkowski, E., Mitchell, C., & Wyeth, A. (2019). Coccolithophore distributions of the North and South Atlantic Ocean. *Deep Sea Research Part I: Oceanographic Research Papers*, *151*, 103066. <https://doi.org/10.1016/j.dsr.2019.06.012>
- Balch, W. M., Drapeau, D. T., Cucci, T. L., Vaillancourt, R. D., Kilpatrick, K. A., & Fritz, J. J. (1999). Optical backscattering by calcifying algae: Separating the contribution of particulate inorganic and organic carbon fractions. *Journal of Geophysical Research*, *104*(C1), 1541–1558. <https://doi.org/10.1029/1998JC900035>
- Balch, W. M., Eppley, R. W., Abbott, M. R., & Reid, F. M. H. (1989). Bias in satellite-derived pigment measurements due to coccolithophores and dinoflagellates. *Journal of Plankton Research*, *11*(3), 575–581. <https://doi.org/10.1093/plankt/11.3.575>
- Balch, W. M., Holligan, P. M., Ackleson, S. G., & Voss, K. J. (1991). Biological and optical properties of mesoscale coccolithophore blooms in the Gulf of Maine. *Limnology and Oceanography*, *36*(4), 629–643. <https://doi.org/10.4319/lo.1991.36.4.0629>
- Balch, W. M., Kilpatrick, K. A., & Trees, C. C. (1996). The 1991 coccolithophore bloom in the central North Atlantic. 1. Optical properties and factors affecting their distribution. *Limnology and Oceanography*, *41*(8), 1669–1683. <https://doi.org/10.4319/lo.1996.41.8.1669>
- Barbieux, M., Uitz, J., Bricaud, A., Organelli, E., Poteau, A., Schmechtig, C., et al. (2018). Assessing the variability in the relationship between the particulate backscattering coefficient and the chlorophyll a concentration from a global biogeochemical-Argo database. *Journal of Geophysical Research: Oceans*, *123*, 1229–1250. <https://doi.org/10.1002/2017JC013030>
- Bellacicco, M., Cornec, M., Organelli, E., Brewin, R. J. W., Neukermans, G., Volpe, G., et al. (2019). Global variability of optical backscattering by non-algal particles from a biogeochemical-Argo data set. *Geophysical Research Letters*, *46*, 9767–9776. <https://doi.org/10.1029/2019GL084078>
- Bishop, J. K. B., & Wood, T. J. (2009). Year-round observations of carbon biomass and flux variability in the Southern Ocean. *Global Biogeochemical Cycles*, *23*, GB2019. <https://doi.org/10.1029/2008GB003206>
- Boss, E., & Pegau, W. S. (2001). Relationship of light scattering at an angle in the backward direction to the backscattering coefficient. *Applied Optics*, *40*(30), 5503–5507. <https://doi.org/10.1364/ao.40.005503>
- Bricaud, A., Bédhomme, A.-L., & Morel, A. (1988). Optical properties of diverse phytoplanktonic species: Experimental results and theoretical interpretation. *Journal of Plankton Research*, *10*(5), 851–873. <https://doi.org/10.1093/plankt/10.5.851>
- Briggs, N., Dall’Olmo, G., & Claustre, H. (2020). Major role of particle fragmentation in regulating biological sequestration of CO₂ by the oceans. *Science*, *367*(6479), 791–793. <https://doi.org/10.1126/science.aay1790>
- Briggs, N., Perry, M. J., Cetinić, I., Lee, C., D’Asaro, E., Gray, A. M., & Rehm, E. (2011). High-resolution observations of aggregate flux during a sub-polar North Atlantic spring bloom. *Deep-Sea Research Part I: Oceanographic Research Papers*, *58*(10), 1031–1039. <https://doi.org/10.1016/j.dsr.2011.07.007>
- Cetinić, I., Perry, M. J., D’Asaro, E., Briggs, N., Poulton, N., Sieracki, M. E., & Lee, C. M. (2015). A simple optical index shows spatial and temporal heterogeneity in phytoplankton community composition during the 2008 North Atlantic bloom experiment. *Biogeosciences*, *12*(7), 2179–2194. <https://doi.org/10.5194/bg-12-2179-2015>

- Claustre, H., Johnson, K. S., & Takeshita, Y. (2020). Observing the global ocean with biogeochemical-Argo. *Annual Review of Marine Science*, 12, 23–48. <https://doi.org/10.1146/annurev-marine-010419>
- Garcia, C. A. E., Garcia, V. M. T., Dogliotti, A. I., Ferreira, A., Romero, S. I., Mannino, A., et al. (2011). Environmental conditions and bio-optical signature of a coccolithophorid bloom in the Patagonian shelf. *Journal of Geophysical Research*, 116, C03025. <https://doi.org/10.1029/2010JC006595>
- Gohin, F., Druon, J. N., & Lampert, L. (2002). A five channel chlorophyll concentration algorithm applied to SeaWiFS data processed by SeaDAS in coastal waters. *International Journal of Remote Sensing*, 23(8), 1639–1661. <https://doi.org/10.1080/01431160110071879>
- Gordon, H. R., Boynton, G. C., Balch, W. M., Groom, S. B., Harbour, D. S., & Smyth, T. J. (2001). Retrieval of coccolithophore calcite concentration from sea WiFS imagery. *Geophysical Research Letters*, 28(8), 1587–1590. <https://doi.org/10.1029/2000GL012025>
- Haëntjens, N., Boss, E., & Talley, L. D. (2017). Revisiting ocean color algorithms for chlorophyll a and particulate organic carbon in the Southern Ocean using biogeochemical floats. *Journal of Geophysical Research: Oceans*, 122, 6583–6593. <https://doi.org/10.1002/2017JC012844>
- Haëntjens, N., Della Penna, A., Briggs, N., Karp-Boss, L., Gaube, P., Claustre, H., & Boss, E. (2020). Detecting mesopelagic organisms using biogeochemical-Argo floats. *Geophysical Research Letters*, 47, e2019GL086088. <https://doi.org/10.1029/2019GL086088>
- Holligan, P. M., Charalampopoulou, A., & Hutson, R. (2010). Seasonal distributions of the coccolithophore, *Emiliania huxleyi*, and of particulate inorganic carbon in surface waters of the Scotia Sea. *Journal of Marine Systems*, 82(4), 195–205. <https://doi.org/10.1016/j.jmarsys.2010.05.007>
- Holligan, P. M., Viollier, M., Harbour, D. S., Camus, P., & Champagne-Philippe, M. (1983). Satellite and ship studies of coccolithophore production along a continental shelf edge. *Nature*, 304, 339–342. <https://doi.org/10.1038/304339a0>
- Holte, J., & Talley, L. (2009). A new algorithm for finding mixed layer depths with applications to Argo data and subantarctic mode water formation*. *Journal of Atmospheric and Oceanic Technology*, 26, 1920–1939. <https://doi.org/10.1175/2009JTECHO543.1.s1>
- Holte, J., Talley, L. D., Gilson, J., & Roemmich, D. (2017). An Argo mixed layer climatology and database. *Geophysical Research Letters*, 44, 5618–5626. <https://doi.org/10.1002/2017GL073426>
- Hopkins, J., Henson, S. A., Painter, S. C., Tyrrell, T., & Poulton, A. J. (2015). Phenological characteristics of global coccolithophore blooms. *Global Biogeochemical Cycles*, 29, 239–253. <https://doi.org/10.1002/2014GB004919>
- Hopkins, J., Henson, S. A., Poulton, A. J., & Balch, W. M. (2019). Regional characteristics of the temporal variability in the global particulate inorganic carbon inventory. *Global Biogeochemical Cycles*, 33, 1328–1338. <https://doi.org/10.1029/2019GB006300>
- Hu, C., Lee, Z., & Franz, B. (2012). Chlorophyll a algorithms for oligotrophic oceans: A novel approach based on three-band reflectance difference. *Journal of Geophysical Research*, 117, C01011. <https://doi.org/10.1029/2011JC007395>
- Lacour, L., Claustre, H., Prieur, L., & D'Ortenzio, F. (2015). Phytoplankton biomass cycles in the North Atlantic subpolar gyre: A similar mechanism for two different blooms in the Labrador Sea. *Geophysical Research Letters*, 42, 5403–5410. <https://doi.org/10.1002/2015GL064540>
- Lide, D. R. (1997). Physical and optical properties of minerals. In D. R. Lide (Ed.), *CRC Handbook of Chemistry and Physics* (pp. 4130–4136). Boca Raton Florida: CRC Press.
- Loisel, H., & Morel, A. (1998). Light scattering and chlorophyll concentration in case 1 waters: A reexamination. *Limnology and Oceanography*, 43(5), 847–858. <https://doi.org/10.4319/lo.1998.43.5.0847>
- Maritorena, S., & Siegel, D. A. (2005). Consistent merging of satellite ocean color data sets using a bio-optical model. *Remote Sensing of Environment*, 94(4), 429–440. <https://doi.org/10.1016/j.rse.2004.08.014>
- Mignot, A., Ferrari, R., & Claustre, H. (2018). Floats with bio-optical sensors reveal what processes trigger the North Atlantic bloom. *Nature Communications*, 9, 190. <https://doi.org/10.1038/s41467-017-02143-6>
- Mitchell, C., Hu, C., Bowler, B., Drapeau, D., & Balch, W. M. (2017). Estimating particulate inorganic carbon concentrations of the Global Ocean from ocean color measurements using a reflectance difference approach. *Journal of Geophysical Research: Oceans*, 122, 8707–8720. <https://doi.org/10.1002/2017JC013146>
- Mohan, R., Mergulhao, L. P., Gupta, M. V. S., Rajakumar, A., Thamban, M., AnilKumar, N., et al. (2008). Ecology of coccolithophores in the Indian sector of the Southern Ocean. *Marine Micropaleontology*, 67(1–2), 30–45. <https://doi.org/10.1016/j.marmicro.2007.08.005>
- Neukermans, G., & Fournier, G. (2018). Optical modeling of spectral backscattering and remote sensing reflectance from *Emiliania huxleyi* blooms. *Frontiers in Marine Science*, 5, 146. <https://doi.org/10.3389/fmars.2018.00146>
- O'Reilly, J. E., Maritorena, S., Mitchell, B. G., Siegel, D. A., Carder, K. L., Garver, S. A., et al. (1998). Ocean color chlorophyll algorithms for SeaWiFS. *Journal of Geophysical Research*, 103(C11), 24,937–24,953. <https://doi.org/10.1029/98JC02160>
- O'Reilly, J. E., Maritorena, S., Siegel, D. A., O'Brien, M. C., Toole, D., Mitchell, B. G., et al. (2000). Ocean color chlorophyll-a algorithms for SeaWiFS, OC2, and OC4: Version 4. *SeaWiFS Postlaunch Technical Report Series*, 11(Part. 3), 9–23.
- Organelli, E., Claustre, H., Bricaud, A., Schmechtig, C., Poteau, A., Xing, X., et al. (2016). A novel near-real-time quality-control procedure for radiometric profiles measured by bio-Argo floats: Protocols and performances. *Journal of Atmospheric and Oceanic Technology*, 33(5), 937–951. <https://doi.org/10.1175/JTECH-D-15-0193.1>
- Patil, S. M., Mohan, R., Shetye, S. S., Gazi, S., Baumann, K. H., & Jafar, S. (2017). Biogeographic distribution of extant coccolithophores in the Indian sector of the Southern Ocean. *Marine Micropaleontology*, 137, 16–30. <https://doi.org/10.1016/j.marmicro.2017.08.002>
- Poulton, A. J., Young, J. R., Bates, N. R., & Balch, W. M. (2011). Biometry of detached *Emiliania huxleyi* coccoliths along the Patagonian shelf. *Marine Ecology Progress Series*, 443, 1–17. <https://doi.org/10.3354/meps09445>
- Read, J. F., Pollard, R. T., & Allen, J. T. (2007). Sub-mesoscale structure and the development of an eddy in the subantarctic front north of the Crozet Islands. *Deep-Sea Research Part II: Topical Studies in Oceanography*, 54(18–20), 1930–1948. <https://doi.org/10.1016/j.dsr2.2007.06.013>
- Rembauville, M., Meilland, J., Ziveri, P., Schiebel, R., Blain, S., & Salter, I. (2016). Planktic foraminifer and coccolith contribution to carbonate export fluxes over the Central Kerguelen plateau. *Deep-Sea Research Part I: Oceanographic Research Papers*, 111, 91–101. <https://doi.org/10.1016/j.dsr.2016.02.017>
- Roesler, C., Uitz, J., Claustre, H., Boss, E., Xing, X., Organelli, E., et al. (2017). Recommendations for obtaining unbiased chlorophyll estimates from in situ chlorophyll fluorometers: A global analysis of WET Labs ECO sensors. *Limnology and Oceanography: Methods*, 15(6), 572–585. <https://doi.org/10.1002/lom3.10185>
- Schmechtig, C., Poteau, A., Claustre, H., D'Ortenzio, F., Dall'Olmo, G., & Boss, E. (2018). Processing BGC-Argo particle backscattering at the DAC level. <https://doi.org/10.13155/39459>
- Stramski, D., Reynolds, R. A., Babin, M., Kaczmarek, S., Lewis, M. R., Röttgers, R., et al. (2008). Relationships between the surface concentration of particulate organic carbon and optical properties in the eastern South Pacific and eastern Atlantic Oceans. *Biogeosciences*, 5(1), 171–201. <https://doi.org/10.5194/bg-5-171-2008>

- Twardowski, M. S., Boss, E., Macdonald, J. B., Pegau, W. S., Barnard, A. H., & Zaneveld, J. R. V. (2001). A model for estimating bulk refractive index from the optical backscattering ratio and the implications for understanding particle composition in case I and case II waters. *Journal of Geophysical Research*, *106*(C7), 14,129–14,142. <https://doi.org/10.1029/2000JC000404>
- Woodward, P. M. (1953). *Probability and information theory, with applications to radar*. New York: McGraw-Hill. Retrieved from catalog.hathitrust.org/Record/000360506
- Xing, X., Briggs, N., Boss, E., & Claustre, H. (2018). Improved correction for non-photochemical quenching of in situ chlorophyll fluorescence based on a synchronous irradiance profile. *Optics Express*, *26*(19), 24,734–24,751. <https://doi.org/10.1364/oe.26.024734>
- Zhang, X., Hu, L., Xiong, Y., Huot, Y., & Gray, D. (2020). Experimental estimates of optical backscattering associated with submicron particles in clear oceanic waters. *Geophysical Research Letters*, *47*, e2020GL087100. <https://doi.org/10.1029/2020GL087100>